Interpolation of G1 Hermite data by C1 cubic-like sparse Pythagorean hodograph splines

Interpolation of G^1 Hermite data by C^1 cubic-like sparse Pythagorean hodograph splines

Rachid Ait-Haddou[1], Carolina Vittoria Beccari[2], Marie-Laurence Mazure[3]

1 - Department of Mathematics and Statistics, King Fahd University of Petroleum and Minerals, Dhahran 31261, Saudi Arabia

2 - Dipartimento di Matematica, Alma Mater Studiorum-Università di Bologna, P.zza di Porta San Donato 5, 40126 Bologna, Italy

3 - Laboratoire Jean Kuntzmann, Université Grenoble-Alpes, CNRS, UMR 5224, 38000 Grenoble, France

The final published version is available online at:

https://doi.org/10.1016/j.cagd.2020.101838

Interpolation of G^1 Hermite data by C^1 cubic-like sparse Pythagorean hodograph splines

Rachid Ait-Haddou[a], Carolina Vittoria Beccari[b], Marie-Laurence Mazure[c]

[a] *Department of Mathematics and Statistics, King Fahd University of Petroleum and Minerals, Dhahran 31261, Saudi Arabia*

[b] *Dipartimento di Matematica, Alma Mater Studiorum–Università di Bologna, P.zza di Porta San Donato 5, 40126 Bologna, Italy*

[c] *Laboratoire Jean Kuntzmann, Université Grenoble-Alpes, CNRS, UMR 5224, 38000 Grenoble, France*

Abstract

Provided that they are in appropriate configurations (tight data), given planar G^1 Hermite data generate a unique cubic Pythagorean hodograph (PH) spline curve interpolant. On a given associated knot-vector, the corresponding spline function cannot be C^1, save for exceptional cases. By contrast, we show that replacing cubic spaces by cubic-like sparse spaces makes it possible to produce infinitely many C^1 PH spline functions interpolating any given tight G^1 Hermite data. Such cubic-like sparse spaces involve the constants and monomials of consecutive degrees, and they have long been used for design purposes. Only lately they were investigated in view of producing PH curves and associated G^1 PH spline interpolants with some flexibility. The present work strongly relies on these recent results.

Keywords: Cubic-like sparse spaces, Pythagorean hodograph splines, G^1 Hermite data, C^1 interpolation

1. Introduction

Pythagorean hodograph planar curves (for short, PH curves) form a remarkable family of parametric polynomial curves with many useful features and characteristics. They have been extensively studied during the last three decades, see [12], [39, 15, 37, 2, 21, 42, 10, 9, 23, 8, 11, 13, 14], and other references therein. In particular, it is well known that, among all cubic planar parametric curves, cubic PH curves can be characterised by geometric properties of their control polygons: equal interior angles and constant ratios between consecutive segments [17]. This geometric characterisation naturally establishes a one-to-one correspondence between the class of all cubic PH curves with obtuse interior angles and G^1 Hermite interpolation problems (two points and associated tangent directions) with appropriate configuration of the data (tight data). Repeated application of this one-to-one correspondence naturally produces a unique PH-spline curve interpolating any given sequence of such G^1 Hermite tight data [1, 36]. However, if the data are associated with a given knot-vector, the unique corresponding G^1 cubic PH spline function cannot be C^1, save for exceptional configurations.

The impossibility of obtaining a C^1 cubic PH spline function interpolating G^1 Hermite data can be viewed as a manifestation of the lack of flexibility of polynomial spaces, due to the fact that no parameter is inherently attached to them. This is the reason why, in many situations, it can be useful to replace them by their most natural generalisations, that is, by Extended Chebyshev spaces [22, 40, 26, 38, 28, 32]. Though more difficult to handle, such spaces present the great advantage to inherently possess parameters which can be used to improve the unique solutions to given problems. Probably the most famous example is provided by the so-called *tension splines* introduced in [41] to eliminate undesired oscillations in cubic spline interpolation. All pieces were taken from the cubic-like Extended Chebyshev space spanned by the functions $1, t, \cosh(at), \sinh(at)$, where a is any positive parameter whose well-known global effect is to produce "C^2 piecewise affine" interpolants at $+\infty$.

In the present paper, the cubic space will be replaced by any space spanned by four functions of the form $1, t^{\ell+1}, t^{\ell+2}, t^{\ell+3}$, where ℓ is a positive integer, which is an Extended Chebyshev space on any interval $[a, b]$ contained in $]0, +\infty[$. The integer ℓ represents the number of missing monomials with respect to the degree $(\ell + 3)$ polynomial space, and for this reason we call it the *sparsity* of this cubic-like space which itself is said to be *sparse*. Sparse spaces are especially interesting for design purposes, because all design algorithms with these spaces are hardly more complicated than with cubic spaces [29, 3]. Moreover, they inherently possess two parameters, first the sparsity parameter ℓ, second the interval parameter b/a related to where they operate, which proved to produce powerful shape effects for spline design [25, 31]. Recently, sparse spaces were used to construct cubic-like PH curves [7], with the advantage of some flexibility resulting from the presence of their two parameters. The most important result to retain from [7] is the characterisation of cubic-like sparse PH curves by geometric properties of their control polygons, which extends the one concerning their cubic counterparts. Along with the presence of parameters, this characterisation will enable us to obtain C^1 cubic-like sparse PH splines based on a fixed knot-vector, interpolating associated G^1 Hermite tight data. This is the object of the present work.

The necessary background on cubic-like sparse spaces and associated splines is briefly presented in Section 2. In particular, we recall why it is recommended that sparse splines be defined after disconnecting the interval parameters from the knot-vector through a positive piecewise affine function. This is crucial for geometric design, for it simultaneously permits to take full advantage of the parameters offered by sparse spaces and overcome their lack of symmetry. The crucial geometric characterisation of cubic-like sparse PH curves by means of their control polygons, and the flexibility they permit, are summarised in Section 3. These results are applied to G^1 Hermite interpolation of tight data by cubic-like sparse PH spline curves in Section 4. As a matter of fact, this question had already been addressed in [7]. However, here, being concerned with C^1 continuity, we are not only interested in the resulting curves, but in cubic-like sparse PH spline functions, based on a given knot-vector associated with the tight data to be interpolated. For this reason, inspired by what is recommended for design, we first have to revisit the definition of cubic-like sparse PH curves. The G^1 Hermite interpolation problem can now be solved via infinitely many different G^1 spline functions preserving the possible symmetry properties of the given tight data. Among this infinitely many solutions, infinitely many are C^1. How to construct the PH segments of such C^1 solutions, one after the other, is explained in Section 5. This progressive method is then illustrated with several examples of tight data taken from classical curves, with special insistence on symmetry preservation. Through one example we also illustrate what can be done when the data are not tight, according to the pre-processing step suggested in [20]. Our results are synthesized and commented in Section 6 with a view to possible future work.

2. Design with sparse cubic-like Müntz spaces and splines

Given any numbers $0 \leqslant r_0 < r_1 < \cdots < r_{n-1} < r_n$, the $(n + 1)$-dimensional space $\mathbb{E}_n$ spanned by the functions t^{r_i}, $i = 0, \ldots, n$, is called a *Müntz space*. The space $\mathbb{E}_n$ is an Extended Chebsyhev space (for short, EC-space) on $]0, +\infty[$, in the sense that any non-zero element of this space vanishes at most n times on $]0, +\infty[$. Suppose that $r_0 = 1$. Then, the (n-dimensional) space $D\mathbb{E}_n$ obtained through the ordinary differentiation D is in turn an EC-space on $]0, +\infty[$, and the EC-space $\mathbb{E}_n$ is said to be *good for design on* $]0, +\infty[$. Indeed, on any positive interval $[a, b]$ (*i.e.*, $0 < a < b$), we can design with the space $\mathbb{E}_n$ instead of the degree n polynomial space, see [27, 34]. Of course we loose the remarkable simplicity of all algorithms in polynomial design, but we gain shape parameters, namely all coefficients $r_1, \ldots, r_n$. *Polynomial Müntz spaces*, corresponding to the special case where the exponents $r_1, \ldots, r_n$, are integers, were fully investigated in [3], see also [34]. An excellent compromise between simplicity and shape effects is obtained when $r_1, \ldots, r_n$ are consecutive integers, for design algorithms are hardly more complicated that in the polynomial case [29, 30, 3]. Such spaces are referred to as *complete Müntz spaces* in [3], see also [6, 5]. From now on, we limit ourselves to the cubic-like case $n = 3$.

2.1. Sparse cubic-like Müntz spaces

The integer $\ell \geqslant 0$ being given, we denote by $\mathbb{M}_\ell$ the four-dimensional complete Müntz space spanned on $\mathbb{R}$ by the functions $1, t^{\ell+1}, t^{\ell+2}, t^{\ell+3}$. For convenience, here, we will refer to it as the *sparse Müntz space* of

sparsity parameter ℓ. The complete symmetric polynomial h_ℓ of degree ℓ in four variables will be an essential tool throughout the paper. It is defined by

$$h_\ell(x_1,x_2,x_3,x_4) \coloneqq \sum_{\substack{\alpha_1,\dots,\alpha_4\geqslant 0\\ \alpha_1+\cdots+\alpha_4=\ell}} {x_1}^{\alpha_1}{x_2}^{\alpha_2}{x_3}^{\alpha_3}{x_4}^{\alpha_4}, \quad x_1,x_2,x_3,x_4\in\mathbb{R}.$$

We shall actually use its normalised version $\widetilde{h}_\ell$, that is,

$$\widetilde{h}_\ell(x_1,x_2,x_3,x_4) := \frac{h_\ell(x_1,x_2,x_3,x_4)}{h_\ell(1,1,1,1)} = \frac{h_\ell(x_1,x_2,x_3,x_4)}{\binom{\ell+3}{3}}.$$

Take any couple (a,b), $0<a<b$. Since $\mathbb{M}_\ell$ is an EC-space good for design on $]0,+\infty[$, it possesses a *Bernstein basis relative to* (a,b) that we denote as $(B_{\ell,0},B_{\ell,1},B_{\ell,2},B_{\ell,3})$. It is the unique sequence of functions in $\mathbb{M}_\ell$ satisfying the following properties:

- *positivity property:* for $i=0,\dots,3$, $B_{\ell,i}$ is positive on $]a,b[$;
- *zero property:* for $i=0,\dots,3$, $B_{\ell,i}$ vanishes exactly i times at a and exactly $(3-i)$ times at b;
- *normalisation property:* the sequence is normalised, in the sense that $B_{\ell,0}(t)+B_{\ell,1}(t)+B_{\ell,2}(t)+B_{\ell,3}(t)=1$ for all $t\in\mathbb{R}$.

For $\ell=0$, $\mathbb{M}_\ell$ is the ordinary cubic space, and $(B_{\ell,0},B_{\ell,1},B_{\ell,2},B_{\ell,3})$ is the standard cubic Bernstein basis relative to (a,b), that we will more classically denote as $(B_0^3,B_1^3,B_2^3,B_3^3)$, with, therefore,

$$B_k^3(t)=\binom{3}{k}\left(\frac{t-a}{b-a}\right)^k\left(\frac{b-t}{b-a}\right)^{3-k}, \quad t\in\mathbb{R}, \quad k=0,\dots,3.$$

The following expressions of Bernstein bases in sparse cubic-like spaces were obtained in [30, 3].

Proposition 1. *Given $0<a<b$, for any positive integer ℓ, the Bernstein basis relative to (a,b) in the space $\mathbb{M}_\ell$ is given by*

$$B_{\ell,k}=\frac{\widetilde{h}_\ell\left((ta)^{[3-k]},(tb)^{[k]},ab\right)}{\widetilde{h}_\ell\left(a^{[4-k]},b^{[k]}\right)\ \widetilde{h}_\ell\left(a^{[3-k]},b^{[k+1]}\right)}\ B_k^3(t), \quad t\in\mathbb{R}, \quad k=0,\dots,3,$$

where the notation $x^{[k]}$ means x repeated k times.

Example 1. As an example, in the simple case $\ell=1$, the explicit expressions giving the Bernstein basis in $\mathbb{M}_1$ are as follows:

$$B_{1,0}(t)=\frac{b+3t}{3a+b}\ B_0^3(t), \qquad B_{1,1}(t)=2\frac{bt+ab+2at}{(a+b)(3a+b)}\ B_1^3(t),$$
$$B_{1,2}(t)=2\frac{2bt+ab+at}{(a+b)(a+3b)}\ B_2^3(t), \qquad B_{1,3}(t)=\frac{a+3t}{a+3b}\ B_3^3(t).$$

Here, designing with cubic-like sparse spaces consists in obtaining planar parametric curves defined by a function

$$P(t)=\sum_{k=0}^{3}B_{\ell,k}(t)P_k, \quad t\in[a,b], \tag{1}$$

where a positive integer ℓ, and $0<a<b$, are given, and with given $P_0,\dots,P_3\in\mathbb{R}^2$ (Bézier points of P relative to (a,b)). Any such function P can be evaluated on $[a,b]$ from its Bézier points $P_0,\dots,P_3$ by three steps of a de Casteljau algorithm [29].

The control polygon $[P_0,P_1,P_2,P_3]$ being selected, the function P in (1) depends on the three parameters ℓ, a,b, $a<b$. By contrast, the resulting parametric curve depends only on two free parameters: on the

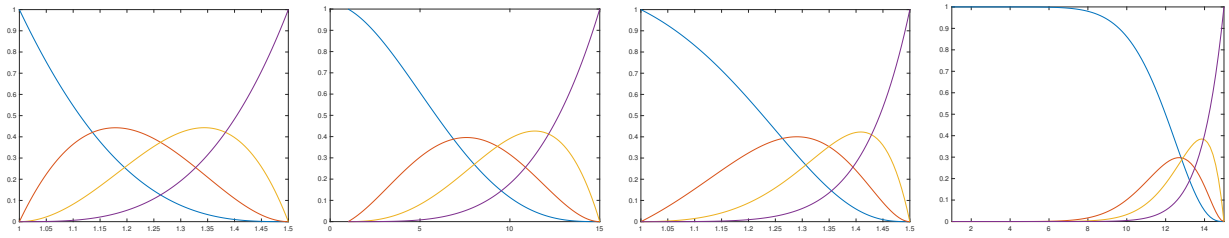

(a) (b) (c) (d)

Figure 1: Bernstein bases of cubic-like sparse spaces: (a) $\ell = 1$, $[a, b] = [1, 1.5]$, (b) $\ell = 1$, $[a, b] = [1, 15]$, (c) $\ell = 10$, $[a, b] = [1, 1.5]$, (d) $\ell = 10$, $[a, b] = [1, 15]$.

one hand, the *sparsity parameter* $\ell \geqslant 1$, on the other *the interval parameter* $\eta := \frac{b}{a} > 1$. Whatever the sparsity parameter, when the interval parameter tends to 1^+, the resulting curve "uniformly converges" (in a mathematical sense to be specified, but this is not our purpose here) to the standard cubic curve with control polygon $[P_0, P_1, P_2, P_3]$ [38]. The two parameters ℓ, η act as shape parameters. Illustrations of their effects on the curves can be found in [7]. In Fig. 1, with $a = 1$, we show the effects on the Bernstein basis resulting from the change of $b > 1$ (*i.e.*, of the interval parameter η) and of the sparsity ℓ. These graphs clearly point out the assymmetry of sparse Bernstein bases, which is one major drawback by comparison with the classical cubic Bernstein basis. Note that this asymmetry increases both with ℓ and η.

We conclude this subsection with the expression of the derivatives of P at the endpoints of the interval $[a, b]$:

$$P'(a) = \frac{3a^\ell}{(b-a)\widetilde{h}_\ell(a,a,a,b)}\,(P_1 - P_0)\,, \quad P'(b) = \frac{3b^\ell}{(b-a)\widetilde{h}_\ell(a,b,b,b)}\,(P_3 - P_2)\,.$$

Out of homogeneity, these formulæ can also be written as follows:

$$P'(a) = \frac{3}{(b-a)\widetilde{h}_\ell(1,1,1,\eta)}\,(P_1 - P_0)\,, \quad P'(b) = \frac{3}{(b-a)\widetilde{h}_\ell(1,1,1,\frac{1}{\eta})}\,(P_3 - P_2)\,, \tag{2}$$

where $\eta = b/a$ is the interval parameter.

2.2. Design with sparse cubic-like splines

The definition of splines based on cubic-like sparse spaces must take into account two difficulties inherent in these spaces: the fact that we have to work on $]0, +\infty[$ and the lack of symmetry.

• Direct definition:

In the case of a bi-infinite sequence t_k, $k \in \mathbb{Z}$, $t_k < t_{k+1}$, of simple knots, a direct definition should require all knots t_k to be positive. Take the simplest situation where the sparsity parameter ℓ is the same everywhere. Then, the analogue of the cardinal case of ordinary cubic splines corresponds to a constant ratio $t_{k+1}/t_k = q > 1$ for all $k \in \mathbb{Z}$. In that case, we have two global shape parameters, $q > 1$ and $\ell > 0$. With the same constant ratio $t_{k+1}/t_k = q$, we can also allow the sparsity parameter ℓ_k to change from interval to interval and serve as a local shape parameter. However, for design with C^2 splines we cannot choose the various sparsities freely, they have to satisfy (see [33])

$$\ell_k - \ell_{k+1} < 2\,\frac{q+1}{q-1}, \quad k \in \mathbb{Z}. \tag{3}$$

In spite of this limitation, such splines can produce efficient shape effects as illustrated in [33]. Such C^2 sparse splines are shown in Fig. 2. A pole P_k representing the knot t_{k+2}, the positive integer indicated close to the segment $[P_k, P_{k+1}]$ is the sparsity ℓ_{k+2} used on the interval $[t_{k+2}, t_{k+3}]$. For the selected sequence of

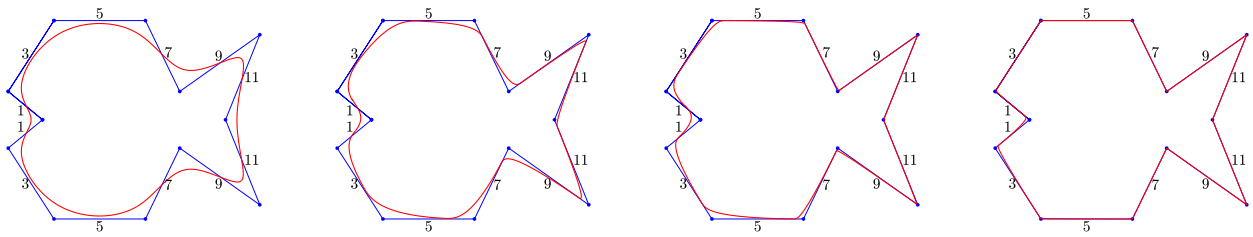

Figure 2: C^2 sparse splines, with positive knots satisfying $t_{k+1}/t_k = q$ for all k, and with the kth piece taken from $\mathbb{M}_{\ell_k}$, where the sparsities ℓ_k are indicated on the control polygons. From left to right: $q = 1.01; 1.5; 2; 5$.

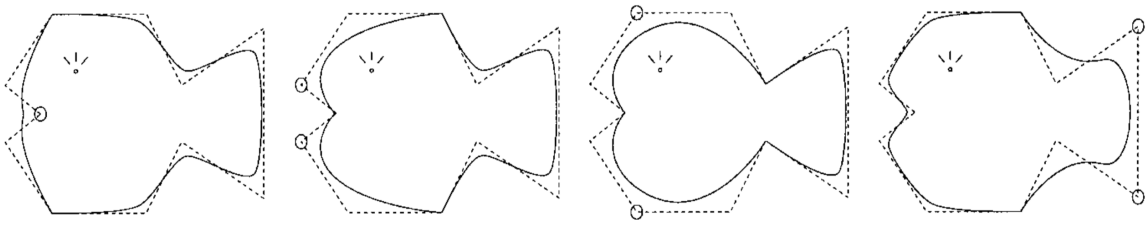

Figure 3: C^1/G^2 sparse splines with knots $t_k := k$ for all k. Everywhere $p_k = 1$, except at the poles indicated by circles, where $p_k = 100$, and with the sparsity equal to 3 in each interval such that $p_k \neq p_{k+1}$.

sparsities, we have $\max_k(\ell_k - \ell_{k+1}) = 2$, and (3) is satisfied for any $q > 1$. When $q = 1.01$, the cubic-like spline curve is close to the standard C^2 cubic spline. Increasing the values of q pushes the spline curve to the control polygon, all the more efficiently as the sparsity increases. Certainly, we have shape preservation, but no symmetry preservation. An obvious inconvenience of this definition of sparse splines is the surprising difference of treatment on the left and right parts of the bi-infinite sequence of knots, since this implies an accumulation of knots at 0^+ and intervals of "infinite" length as we move to the right.

However, the major drawback is that, in case the knots are given, we cannot take any benefit from the successive interval parameters which are derived from the knots. This is why sparse cubic-like splines (and more generally Müntz splines) are more usually defined differently, as we will now explain.

• More convenient framework:

A bi-infinite sequence of knots t_k, $k \in \mathbb{Z}$, is given, with $t_k < t_{k+1}$ for all k as the only requirement, along with a bi-infinite sequence of positive numbers p_k, $k \in \mathbb{Z}$. To introduce the section-space $\mathbb{E}_k$ on $[t_k, t_{k+1}]$, two cases are to be considered, see [25, 35, 31].

1. Suppose that $p_k = p_{k+1}$: then the space $\mathbb{E}_k$ is the restriction to $[t_k, t_{k+1}]$ of the cubic polynomial space.
2. Suppose that $p_k \neq p_{k+1}$: then we select a non-negative integer ℓ_k, and the section-space $\mathbb{E}_k$ on $[t_k, t_{k+1}]$ is obtained from the sparse cubic-like space $\mathbb{M}_{\ell_k}$ restricted to the positive interval $I_k := [\min(p_k, p_{k+1}), \max(p_k, p_{k+1})]$, through the affine change of variable $\vartheta_k : [t_k, t_{k+1}] \longrightarrow I_k$ such that $\vartheta_k(t_i) = p_i$ for $i = k, k+1$, that is,

$$\vartheta_k(x) := \frac{t_{k+1} - x}{t_{k+1} - t_k}\, p_k + \frac{x - t_k}{t_{k+1} - t_k}\, p_{k+1}, \quad x \in [t_k, t_{k+1}].$$

Associated with these data, a sparse spline is a continuous function $S :]\inf_k(t_k), \sup_k(t_k)[\longrightarrow \mathbb{R}$, such that, for each $k \in \mathbb{Z}$, S coincides with a function $F_k \in \mathbb{E}_k$ on $[t_k, t_{k+1}]$. Considering all knots as simple, the definition of a spline space will be completed by the relations between left and right first and second derivatives at all knots, so as to produce C^2 splines or, more generally, order two geometrically continuous splines, in a way convenient for design [31].

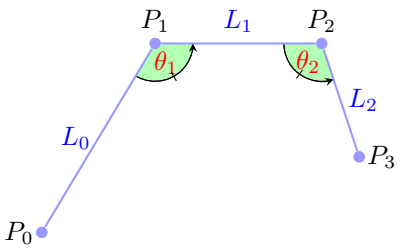

Figure 4: Labelling of relevant geometric data related to a control polygon $[P_0, P_1, P_2, P_3]$.

Examples of such splines are shown in Figure 3, directly copied from [31]. The knots are defined by $t_k := k$ for all $k \in \mathbb{Z}$, and all p_k are equal to 1, except at some knots indicated by circles where $p_k = 100$. The sparsity is equal to 3 in all intervals where we do not have ordinary cubic segments. The splines are C^1 and G^2, and they differ only from the places of the circles. More details on the connection matrices used and more examples can be found in [31]. Unlike the splines in Fig. 2, here, in addition to shape preservation, we do have symmetry preservation due to the values of the positive numbers p_k being selected symmetrically. The reason why it is so will be made clear in the next sections.

3. Cubic-like sparse PH curves

In this section we need to briefly explain how to recognise that a given cubic-like sparse curve is a PH curve, and how to construct such PH curves. The results summarised below were obtained in [7].

3.1. Characterisation of cubic-like sparse PH curves

Recall that a parametric curve defined by a polynomial function $P(t) = (x(t), y(t))$, $t \in [a, b]$, is said to be a Pythagorean-Hodograph (PH) curve if and only if there exists a real polynomial σ such that

$$x'^2(t) + y'^2(t) = \sigma^2(t), \quad \text{for all} \quad t \in [a, b]. \tag{4}$$

Subsequently, given a planar polygon $[P_0, P_1, P_2, P_3]$, we use the notations L_0, L_1, L_2, for the lengths of its segments, and θ_1, θ_2 for its angles, as indicated in Fig. 4. A sparsity $\ell > 0$ being selected, along with a positive interval $[a, b]$, we consider the associated cubic-like sparse curve produced by the function $P : [a, b] \longrightarrow \mathbb{R}^2$ defined in (1). Below we recall when it is a PH curve [7].

Theorem 2. *The cubic-like sparse curve produced by the function P defined in (1) is a PH curve if and only if the polygon $[P_0, P_1, P_2, P_3]$ satisfies the conditions*

$$\theta_1 = \theta_2 \qquad \text{and} \qquad (L_1)^2 = \psi_\ell(\eta)\, L_0\, L_2, \tag{5}$$

where $\eta = b/a$ is the interval parameter, and where

$$\psi_\ell(\eta) = \frac{h_\ell(1, 1, \eta, \eta)^2}{h_\ell(1, 1, 1, \eta) h_\ell(1, \eta, \eta, \eta)}. \tag{6}$$

Remark 1. For $\ell = 0$, the quantity $\psi_\ell(\eta)$ is identically equal to 1. In that case, the right part of (5) becomes $(L_1)^2 = L_0\, L_2$. Therefore, for $\ell = 0$, the conditions (5) yield the well-known characterisation of cubic PH curves in terms of their control polygons [17]. In that case only, the characterisation does not involve the interval. [1]

[1] The notion of PH curves was extended to cycloidal curves in [24], where the authors also established a characterisation of PH cycloidal curves similar to the classical condition $\theta_1 = \theta_2$ and $(L_1)^2 = L_0\, L_2$.

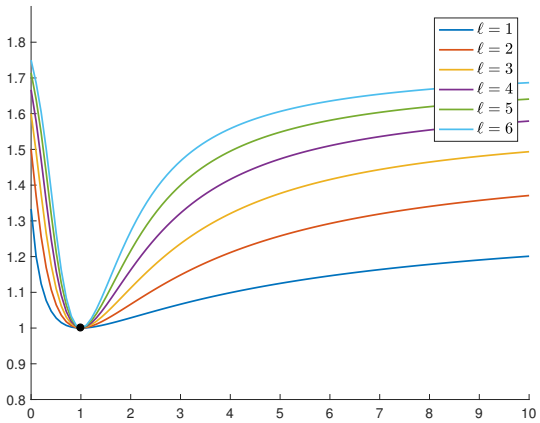

Figure 5: Graph of the function ψ_ℓ defined by (6) on $[0, +\infty[$ for various values of the integer $\ell \geqslant 1$.

The function ψ_ℓ is thus a crucial tool for cubic-like sparse PH curves. Let us remind the reader about its variations, see Fig. 5.

Theorem 3. *Given $\ell \geqslant 1$, the function ψ_ℓ defined by the expression (6) on $[0, +\infty[$ satisfies*

$$\psi_\ell\left(\frac{1}{\eta}\right) = \psi_\ell(\eta) \quad \textit{for all } \ell > 0, \tag{7}$$

and is strictly increasing on $[1, +\infty[$ from 1 to $\frac{2\ell+2}{\ell+2}$.

Remark 2. The difficult part in the proof of Theorem 3 consists in showing that the function ψ_ℓ is strictly decreasing on $[0, 1]$ [7]. Its main originality is to make it necessary to consider some Müntz spaces on $[0, 1]$, and to apply to them design techniques as developed in [4], although they are not EC-spaces on this interval. For this reason, they cannot be handled through Bernstein bases, but through Gelfond-Bernstein bases [18, 19]. Note that the asymptotic value $\frac{2\ell+2}{\ell+2}$ is strictly increasing with ℓ and its limit when $\ell \to +\infty$ is equal to 2. Take any $\alpha \in]1, 2[$, and any integer ℓ such that $\frac{2\ell+2}{\ell+2} > \alpha$, that is, such that $\ell > \frac{2\alpha-2}{2-\alpha}$. Then, there is a unique $\eta > 1$ such that $\psi_\ell(\eta) = \alpha$.

3.2. Geometric construction of cubic-like sparse PH curves

Let us start with a non-degenerate triangle $[A, B, C]$, with $\|C-B\| \geqslant \|A-B\|$ (the case $\|C-B\| \leqslant \|A-B\|$ can be treated similarly). Let C' be the point located on the segment $[B, C]$ such that $\|C' - B\| = \|A - B\|$. Selecting a point $E \in]A, B[$, and a point $F \in]B, C[$, consider the cubic-like sparse curve defined in (1) with control polygon $[P_0, P_1, P_2, P_3]$ given by

$$P_0 := A, \quad P_1 := E, \quad P_2 := F, \quad P_3 := C. \tag{8}$$

For this polygon to satisfy the left part of (5) it is necessary and sufficient to require the segment $[E, F]$ to be parallel to $[A, C']$. Subsequently, we assume this to be satisfied. With each point E in the segment $[B, A]$, we then associate the quantity

$$\alpha(E) := \frac{L_1(E)^2}{L_0(E)\, L_2(E)} := \frac{\|P_2 - P_1\|^2}{\|P_1 - P_0\|\ \|P_3 - P_2\|},$$

called the *polygon parameter* of $[P_0, P_1, P_2, P_3]$. The values of this function α strictly increase from 0 to $+\infty$ as E ranges from B to A. Conversely, given $\alpha \in [0, +\infty[$ (on purpose to avoid too many notations, we

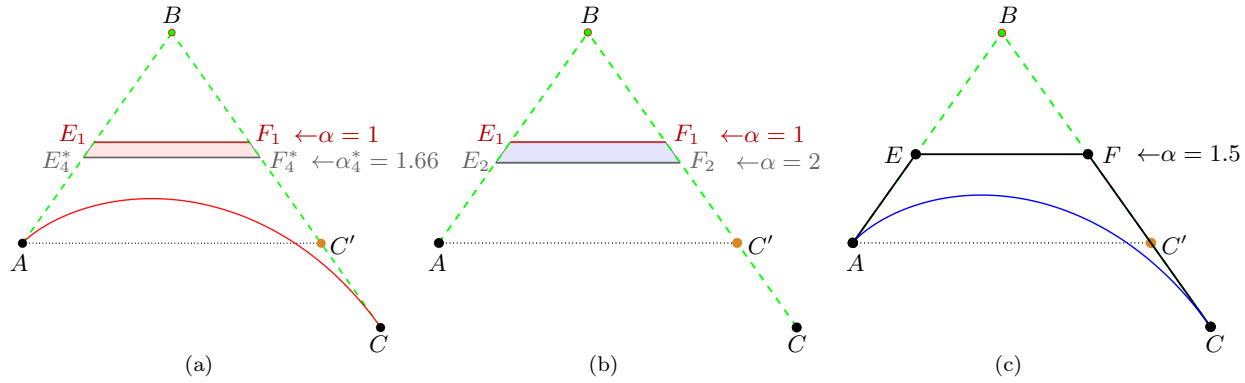

Figure 6: Left: for $\ell = 4$, the red region corresponds to $\alpha = 1$ and $\alpha_4^* = 1.6667$ and the red curve is obtained with $\alpha = 1.6$ and corresponding $\eta \approx 12.7813$. Center: The purple region represents the allowed band $E \in [E_1, E_2]$, $F \in [F_1, F_2]$; Right: $\ell = 3$ and $\eta \approx 10.5956$.

use the same symbol for the function α and its values) the unique point E in the segment $[B, A[$ such that $\alpha(E) = \alpha$ is given by

$$\|E - A\| = \frac{2ab^2}{ac\alpha + 2b^2 + \sqrt{a\alpha\big[ac^2\alpha + 4b^2(a+c)\big]}}, \tag{9}$$

where, in this formula and only there, the letters a, b, c have the following meaning

$$a := \|A - B\|, \quad b := \|C' - A\|, \quad c := \|C - C'\|.$$

We denote by E_1 and E_2 the two points on $]B, A[$ such that

$$\alpha(E_1) = 1, \qquad \alpha(E_2) = 2.$$

Moreover, on the open segment $]E_1, E_2[$, we can place the monotonic sequence of points E_ℓ^* characterised by

$$\alpha(E_\ell^*) = \alpha_\ell^*, \qquad \text{with } \alpha_\ell^* := \frac{2\ell + 2}{\ell + 2}, \quad \ell \geqslant 1,$$

for which therefore $\|E_\ell^* - A\|$ is given by (9), with $\alpha = \alpha_\ell^*$. Below we summarise two possible interpretations of Theorems 2 and 3 for the obtention of cubic-like sparse PH curves.

• PH-curves from sparsity:

Any given positive integer ℓ being selected, the triangle $[A, B, C]$ produces infinitely many cubic-like PH-curves with sparsity parameter ℓ. For any of them, the control polygon $[P_0, P_1, P_2, P_3]$ in (8) is characterised by either the point $E \in]E_1, E_\ell^\star[$, or its polygon parameter $\alpha \in]1, \alpha_\ell^\star[$, or its interval parameter $\eta \in]1, +\infty[$, the one-to-one correspondences between E, α, η being through (9), with

$$\alpha = \psi_\ell(\eta). \tag{10}$$

Each corresponding PH curve itself can be obtained as the image of the function P in (1) on any positive interval $[a, b]$ such that $\frac{b}{a} = \eta$. The evolution of the PH curve as α ranges in $]1, \alpha_\ell^*[$ cannot be impressive, for the control polygons are limited by a narrow band. This narrow band is shown in Fig. 6, (a), for $\ell = 4$, and with therefore $\alpha_\ell^* = \frac{5}{3} \approx 1.66$. The red curve is obtained with $\alpha = 1.6$. The interval parameter is thus defined by $\psi_4(\eta) = 1.6$, which gives $\eta \approx 12.7813$.

• PH-curves from polygon parameter:

The discussion is now in terms of the polygon parameter $\alpha \in [0, +\infty[$, or, as well, in terms of the point $E \in [B, A[$ associated with α through (9), producing the polygon $[P_0, P_1, P_2, P_3]$ as in (8).

1. Assume that $\alpha = 1$, *i.e.*, $E = E_1$. Then, the polygon $[P_0, P_1, P_2, P_3]$ produces exactly one PH curve, which is the cubic curve with control polygon $[P_0, P_1, P_2, P_3]$, whatever the interval $[a, b]$ ($\ell = 0$).
2. Assume that $1 < \alpha < 2$, *i.e.*, that E is located in the open interval $]E_1, E_2[$. Then, the corresponding polygon $[P_0, P_1, P_2, P_3]$ produces infinitely many PH curves. More precisely, for each integer $\ell > \frac{2\alpha-2}{2-\alpha}$ (see Remark 2), the cubic-like curve with sparsity ℓ, and control polygon $[P_0, P_1, P_2, P_3]$ is a PH curve. Once ℓ chosen, the associated interval parameter η is given by (10).
3. Assume that $\alpha < 1$ (*i.e.*, $E \in]B, E_1[$) or $\alpha \geqslant 2$ (*i.e.*, $E \in [E_2, A[$). Then, whatever the integer $\ell \geqslant 0$ and whatever $\eta > 1$, the sparse cubic-like curve with sparsity ℓ, interval parameter η and control polygon $[P_0, P_1, P_2, P_3]$ is not a PH curve.

This discussion is summarised in Fig. 6, (b), where the purple band represents the region where to choose segments $[E, F]$ parallel to $[A, C']$ producing PH curves. In Fig. 6, (c), we consider the polygon corresponding to $\alpha = 1.5$. In that case $\frac{2\alpha-2}{2-\alpha} = 2$. Therefore, this fixed polygon generates infinitely many cubic-like sparse PH curves, with sparsities $\ell > 2$. The blue curve is obtained with $\ell = 3$. The associated interval parameter is given by $\psi_3(\eta) = 1.5$, which corresponds to $\eta \approx 10.5956$.

4. Interpolation of G^1 Hermite data with sparse cubic-like PH spline curves: a revisit

By *cubic-like sparse PH-spline curves* we mean spline curves composed of cubic-like sparse PH segments, the sparsity being allowed to depend on the segment and even to be zero at some places. By comparison, by *cubic PH-spline curves* we mean that all segments are standard cubic PH curves. In this section we revisit the G^1 Hermite interpolation by cubic-like sparse PH-spline curves already addressed in [7].

4.1. Cubic-like sparse PH curves to interpolate G^1 Hermite data

The construction of cubic-like sparse PH curves from a non-degenerate triangle can be interpreted as the construction of cubic-like PH curves interpolating G^1 data (interpolation of two points plus oriented tangents) in convenient configurations. More precisely, given two points $q_0, q_1 \in \mathbb{R}^2$ and two associated unit tangent directions d_0, d_1, we assume that these data are *tight*, *i.e.*, they satisfy

$$\begin{aligned} \det(d_0, q_1 - q_0) < 0, \qquad & \det(q_1 - q_0, d_1) < 0, \\ \langle d_0, q_1 - q_0 \rangle > 0, \qquad & \langle q_1 - q_0, d_1 \rangle > 0. \end{aligned} \tag{11}$$

Conditions (11) mean that the angles $\angle(q_1 - q_0, d_0)$ and $\angle(d_1, q_1 - q_0)$ both belong to $]0, \frac{\pi}{2}[$. They ensure the existence of a unique point $q_{0,1}$ common to the two lines passing by q_0, q_1 with directions d_0, d_1, respectively. The previous analysis can be applied to the triangle $[A, B, C] = [q_0, q_{0,1}, q_1]$, to obtain infinitely many PH curves with extreme points A and C and unit tangent vectors $d_0 = \lambda_0(B - A)$, and $d_1 = \lambda_1(C - B)$, for some $\lambda_0, \lambda_1 > 0$. Let us recall that the well-known properties of EC-spaces good for design make it impossible to have either λ_0 or λ_1 equal to 0 [31].

Consider a number of points $q_k \in \mathbb{R}^2$, $k = 0, \ldots, r + 1$, and associated unit tangent directions d_k, $k = 0, \ldots, r + 1$, such that any two consecutive pairs (q_k, d_k), (q_{k+1}, d_{k+1}) are tight in the sense of (11) (for short, we will say that the data are tight). Repeating the process provides us with infinitely many G^1 cubic-like sparse PH-spline curves interpolating the data. More precisely, if we avoid cubic segments, this provides us with infinitely possible triplets $(\ell_k, \alpha_k, \eta_k)$, $k = 0, \ldots, r$, where the integer $\ell_k \geqslant 1$ is the sparsity of the kth segment, $\alpha_k \in]1, 2[$, $\eta_k > 1$, are its polygon and interval parameters, linked by the relations

$$\psi_{\ell_k}(\eta_k) = \alpha_k, \qquad k = 0, \ldots, r.$$

For more details, see [7]. To precisely associate with such a spline curve a spline function, any positive number t_0 being selected, the next knots must be chosen so as to satisfy

$$\frac{t_{k+1}}{t_k} = \eta_k, \qquad k = 0, \ldots, r. \tag{12}$$

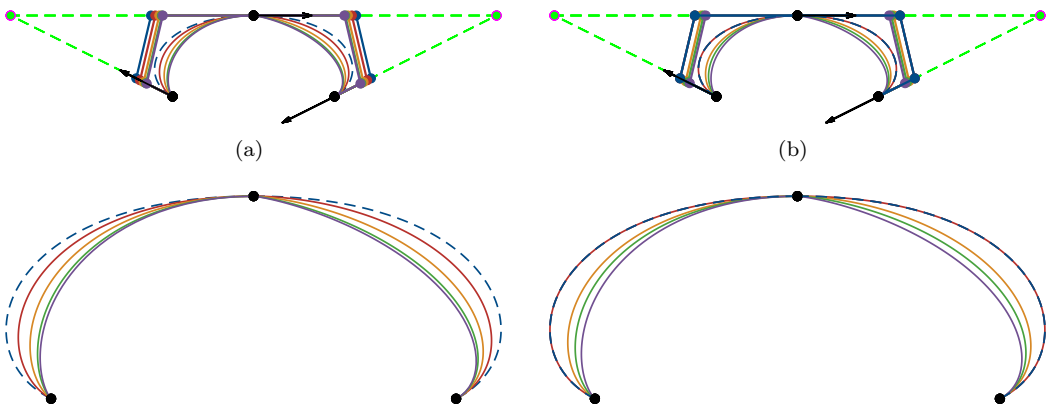

Figure 7: (a) and (c): $\eta_0 = \eta_1 = 15$ and $\ell_0 = \ell_1 = 1, 3, 8, 15$; (b) and(d): $\ell_0 = \ell_1 = 8$ and $\eta_0 = \eta_1 = 1.01, 2, 3, 15$. In all the figures, the dashed blue curve is the ordinary cubic PH-spline.

Conversely, if a strictly increasing sequence t_k, $k = 0, \ldots, r+1$, of positive knots is given, for each sequence of sparsities $\ell_k \geqslant 1$, $k = 0, \ldots, r$, the relations (12) provide us with the sequence of interval parameters $\eta_k > 1$, $k = 0, \ldots, r$, and therefore with the corresponding cubic-like sparse PH segments.

Contrary to cubic PH-spline curves, we can thus interpolate G^1 data with some flexibility. Illustrations of this flexibility can be found in [7]. Nevertheless, supposing that the sequence of knots is imposed, only the sparsities are free parameters. In that case, each choice of the successive sparsities $\ell_0, \ldots, \ell_r$, produces a unique spline function on $[t_0, t_{r+1}]$. This spline function is G^1 and it will be C^1 only by exception. This is known to also be true when we interpolate G^1 tight data with cubic PH-spline curves.

The question of obtaining a C^1 PH-spline function will be addressed in Section 5. Prior to that, it is necessary to provide new insights into interpolation of G^1 Hermite data by cubic-like sparse PH-spline curves. This is motivated by the fact that the advantages / inconveniences presented by the interpolating splines described in the previous subsection by comparison with the cubic case, are similar to those described in Section 2, namely: more flexibility but no symmetry preservation. To clarify the question of symmetry, take three pairs of G^1 data (q_k, d_k), $k = 0, 1, 2$, satisfying two by two the tightness conditions (11), and assume the two triangles $[q_0, q_{0,1}, q_1]$ and $[q_1, q_{1,2}, q_2]$ to be symmetric of each other, as in Fig. 7. While the unique resulting cubic PH-spline curve interpolating these G^1 data is symmetric (dashed blue curves in Fig. 7), no choice of the sparsities $\ell_0, \ell_1 \geqslant 1$, and of the interval parameters $\eta_0, \eta_1 > 1$ will yield a symmetric cubic-like sparse PH-spline curve. Though not spectacular, the lack of symmetry can be observed in the examples shown in Fig. 7, where we present both symmetric control polygons (up), and the zoomed associated non-symmetric sparse PH-spline curves (down). Moving back from the details, one can see that, as ℓ or η increases, the right half of the curve is crushed by comparison to the left one (concerning the lack of symmetry of sparse spaces, see Fig. 3 in [7]). In order to ensure symmetry preservation, we will change the spaces in which to build the interpolating segments. The underlying idea, already presented in Section 2.2 is natural when dealing with Müntz splines. It will present the additional advantage to both get rid of the positivity constraint for the knots, and increase the flexibility of the resulting curves.

4.2. Sparse cubic-like spaces: a modified definition

Starting again with one pair of tight data (q_0, d_0), (q_1, d_1), we will analyse the corresponding G^1 Hermite interpolation problem differently, by analogy to what is done for design, as recalled in Section 2.2. We first choose any non-trivial closed bounded real interval I, say $I = [0, 1]$. For each sparsity $\ell \geqslant 1$ and each pair (p_0, p_1) of positive numbers, with $p_0 \neq p_1$, we denote by $\mathbb{M}(\ell; p_0, p_1)$ the restriction of the space $\mathbb{M}_\ell$ to the interval

$$[a, b] := [\min(p_0, p_1), \max(p_0, p_1)] .$$

The space $\mathbb{E}(\ell; p_0, p_1)$ in which we will interpolate is obtained from $\mathbb{M}(\ell; p_0, p_1)$ via the change of variable $\vartheta : I \longrightarrow [a, b]$ such that

$$\vartheta(0) = p_0, \qquad \vartheta(1) = p_1, \qquad \vartheta \text{ is affine on } [0, 1]. \tag{13}$$

In other words,

$$\mathbb{E}(\ell; p_0, p_1) \coloneqq \{F \circ \vartheta \mid F \in \mathbb{M}(\ell; p_0, p_1)\}. \tag{14}$$

As the image of an EC-space good for design on $[a, b]$ through a change of variable, $\mathbb{E}(\ell; p_0, p_1)$ is an EC-space good for design on $I = [0, 1]$, in which the Bernstein basis / Bézier points relative to $(0, 1)$ are obtained from the Bernstein basis / Bézier points relative to (a, b) in $\mathbb{M}(\ell; p_0, p_1)$. We need to be more precise on this question. Given $P \in \mathbb{M}(\ell; p_0, p_1)^2$, with Bézier points relative to (a, b) denoted by $P_0, \ldots, P_3$, let Q_0, Q_1, Q_2, Q_3 be the Bézier points relative to $(0, 1)$ of the function $Q := P \circ \vartheta \in \mathbb{E}(\ell; p_0, p_1)^2$. Two cases are to be considered:

1. if $p_0 < p_1$, then $[a, b] = [p_0, p_1]$ and $(Q_0, Q_1, Q_2, Q_3) = (P_0, P_1, P_2, P_3)$;
2. if $p_0 > p_1$, then $[a, b] = [p_1, p_0]$ and $(Q_0, Q_1, Q_2, Q_3) = (P_3, P_2, P_1, P_0)$.

In other words, the polygon defined by the Bézier points is the same for F and G, but depending on the case it is in the reverse order.

In the sparse space $\mathbb{M}(\ell; p_0, p_1)$, as usual the interval parameter is the ratio $\eta := b/a > 1$. It is equal either to p_1/p_0 (first case) or to p_0/p_1 (second case). For the sake of simplicity, though it is an abuse of language, we will define *the interval parameter in the space* $\mathbb{E}(\ell; p_0, p_1)$ as the ratio

$$\eta := \frac{p_1}{p_0} \in]0, +\infty[\setminus \{1\}.$$

The space $\mathbb{E}(\ell; p_0, p_1)$ is what we now consider a cubic-like sparse space. The interval is fixed and the interval parameter is no longer deduced from it. Whether this parameter η is less or bigger than 1, we always have (see (2))

$$Q'(0) = \frac{3}{\varphi_\ell(\eta)}(Q_1 - Q_0), \qquad Q'(1) = \frac{3}{\varphi_\ell\left(\frac{1}{\eta}\right)}(Q_3 - Q_2), \tag{15}$$

where the function φ_ℓ is defined by

$$\varphi_\ell(x) \coloneqq \widetilde{h}_\ell(1, 1, 1, x), \quad x \geqslant 0. \tag{16}$$

In itself, the space $\mathbb{E}(\ell; p_0, p_1)$ does not possess more symmetry properties than the space $\mathbb{M}(\ell; p_0, p_1)$. Indeed, a symmetric control polygon $[Q_0, Q_1, Q_2, Q_3]$ produces two sparse cubic-like curves, which are not symmetric, but are symmetric of each other, one lies in the space $\mathbb{E}(\ell; p_0, p_1)$ (with interval parameter η) and the other in the space $\mathbb{E}(\ell; p_1, p_0)$ (with interval parameter $1/\eta$). Observe that this was already one major underlying reason why the splines in Fig. 3 preserve the symmetry of the data.

From (4) it is clear that being a PH-curve is the same in $\mathbb{E}(\ell; p_0, p_1)^2$ or in $\mathbb{M}(\ell; p_0, p_1)^2$. It is therefore characterised by the same conditions (5) on angles and lengths of the control polygon. These conditions are simultaneously satisfied in $\mathbb{E}(\ell; p_0, p_1)$ and $\mathbb{E}(\ell; p_1, p_0)$. We will keep the same terminology *cubic-like sparse PH-curves* in these spaces. The discussion about the construction of such curves from non-degenerate triangles can also be developed exactly as previously, simultaneously in $\mathbb{E}(\ell; p_0, p_1)$ and $\mathbb{E}(\ell; p_1, p_0)$. Note that, if α is the polygon parameter of $[Q_0, Q_1, Q_2, Q_3]$, the corresponding interval parameters are the two solutions to the equation $\psi_\ell(\eta) = \alpha$ (see Fig. 5).

So far, to define the cubic-like sparse space $\mathbb{E}(\ell; p_0, p_1)$ on $[0, 1]$, we have assumed that $p_0 \neq p_1$. As in Section 2.2, when $p_0 = p_1$, the space $\mathbb{E}(\ell; p_0, p_1)$ is naturally defined as the cubic space on $[0, 1]$, with therefore $\ell = 0$, and "interval parameter" $\eta = 1$. Note that the formulæ (15) are valid in that case too.

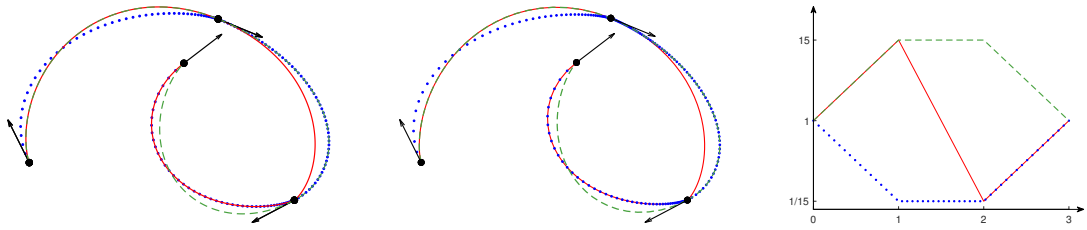

Figure 8: G^1 Cubic-like sparse PH splines with sparsity equal to 3 (left) and 7 (middle) in each non standard cubic section, corresponding to the piecewise affine functions shown on the right.

4.3. Advantages

The advantages of working with spaces of the form $\mathbb{E}(\ell; p_0, p_1)$ rather than directly in $\mathbb{M}_\ell$ are obvious as soon as we are interested in splines. They are actually similar to those encountered for design, as briefly reminded in Section 2.2.

• More flexibility:

Given again a sequence of G^1 Hermite tight data (q_k, d_k), $k = 0, \ldots, r+1$, we reformulate the problem of constructing a cubic-like sparse PH spline function S based on any given strictly increasing sequence of knots t_k, $k = 0, \ldots, r+1$, which interpolates these data. The G^1 Hermite interpolation problem can be stated as follows:

Find a spline $S : [t_0, t_{r+1}] \longrightarrow \mathbb{R}^2$ *satisfying the conditions below:*

1) $S(t_k) = q_k$ *for* $k = 0, \ldots, r+1$;

2) *for each* $k = 0, \ldots, r$, *(resp., for each* $k = 1, \ldots, r+1$*), there exists a positive* λ_k^+ *(resp.,* λ_k^-*) such that* $S'(t_k^+) = \lambda_k^+ d_k$ *(resp.,* $S'(t_k^-) = \lambda_k^- d_k$*);* (17)

3) *for each* $k = 0, \ldots, r$, *the restriction of* S *to* $[t_k, t_{k+1}]$ *produces a cubic-like sparse PH curve,*

where t_k^+, t_k^-, mean t_k considered as belonging to $[t_k, t_{k+1}]$, $[t_{k-1}, t_k]$, respectively.

By comparison to what we described in Section 4.1. the disconnection between the intervals on which the cubic-like sparse spaces are defined and their interval parameters, permits more flexibility to solve the problem above, as stated below.

Theorem 4. *Given any planar tight data* (q_k, d_k), $k = 0, \ldots, r+1$, *the interpolation problem (17) has infinitely many solutions.*

Proof. Associated with the sequence of knots, we have at our disposal two sequences of parameters:

– a sequence p_k, $k = 0, \ldots, r+1$; of positive numbers;
– a sequence of sparsities $\ell_k \geqslant 0$, $k = 0, \ldots, r$.

These parameters can be chosen freely, except for the requirement that $\ell_k = 0$ if and only if $p_k = p_{k+1}$. For each k, we denote by $\mathbb{E}(\ell_k; p_k, p_{k+1})$ the sparse cubic-like space defined on the interval $[t_k, t_{k+1}]$ as we did in the previous subsection for $\mathbb{E}(\ell; p_0, p_1)$ on $[0, 1]$.

Suppose the sequence of sparsities to be selected. If $\ell_k = 0$ for $k = 0, \ldots, r$ (or, equivalently, if $p_0 = p_1 = \cdots = p_{r+1}$), there exists only one cubic spline S meeting all requirements in (17). By contrast, as soon as at least one ℓ_k is greater than or equal to 1, we have infinitely many different possible S, in one-to-one correspondence with the infinitely many possible non-constant sequences of positive numbers p_k, $k = 0, \ldots, r+1$, with $p_0 = 1$. This readily follows from the discussion in Section 3.2 adapted to the sparse spaces $\mathbb{E}(\ell_k; p_k, p_{k+1})$. □

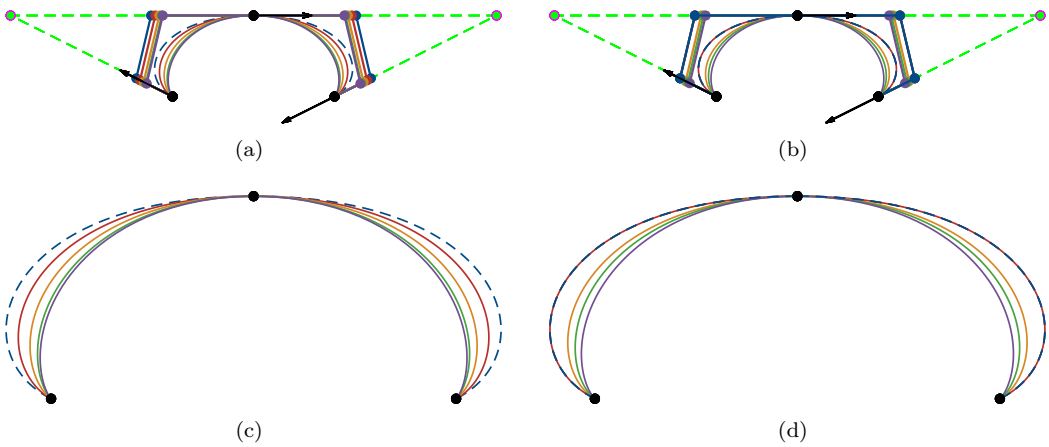

Figure 9: Symmetry preservation with G^1 interpolation by sparse PH-splines based on the knots $t_k = k$, $k = 0, 1, 2$, with $p_0 = p_2 = 1$. In (a) and (c) $p_1 = 15$, and (continuous lines) $\ell_0 = \ell_1 = 1; 3; 8; 15$. In (b) and (d), $\ell_0 = \ell_1 = 8$, and $p_1 = 1.01; 2; 3; 15$. In all the figures, the dashed blue curve is the ordinary cubic PH curve.

Theorem 4 is illustrated in Fig. 8, with $r = 2$, and $t_k = k$ for $k = 0, 1, 2, 3$. For $(\ell_0, \ell_1, \ell_2) = (3, 0, 3)$ and $p_0 = 1$ we can take any positive p_1, p_2, p_3 provided that $p_1 = p_2$. Such possibilities are represented by the graphs of the piecewise affine functions $p : [t_0, t_3] \longrightarrow \mathbb{R}$ such that $p(t_k) = p_k$, for $k = 0, 1, 2, 3$. The two dotted blue and dashed green broken lines (Fig. 8, right) are such examples, and the graphs of the corresponding splines S are represented in accordance with them (Fig. 8, left). Observe that the central segments are identical in both cases: they are cubic PH segments. As for the red curve, it is the graph of the spline S obtained with the continuous red broken line and $\ell_0 = \ell_1 = \ell_2 = 3$. Its first (resp., last) segment coincides with the dashed green first (resp., dotted blue last) curve segment. In Fig. 8, middle, we can see the same illustrations with the sparsity 3 replaced by 7.

• Symmetry preservation:

Take the same three pairs of tight data presenting symmetry properties as in Fig. 7. With $t_k = k$ for $k = 0, 1, 2$, we want to construct cubic-like sparse PH-splines S interpolating these G^1 Hermite data, but we now want to preserve their symmetry. This is extremely easy to obtain, and there are infinitely many solutions to this problem. We simply have to take $p_0 = p_2 = 1$ and complete with any positive number p_1, and then choose appropriate values for the sparsity $\ell_0 = \ell_1$. For $p_1 = 1$, S is an ordinary cubic spline (*i.e.*, $\ell_0 = \ell_1 = 0$) corresponding to the dashed blue curve. The other curves represent sparse PH-curves, which, unlike those in Fig. 7, are perfectly symmetric. We show the successive symmetric control polygons (up) and we zoom on the curves (down) to make the symmetry preservation clear. In Fig. 9, (a) and (c), we take $p_1 = 15$, which means that the interval parameter is $\eta_0 = 15$ for the first segment, and $\eta_1 = \frac{1}{15}$ for the second one. The various spline curves are obtained successively with $\ell_0 = \ell_1 = 1; 3; 8; 15$. For each of these values, in both segments the control polygons have polygon parameter $\psi_{\ell_0}(15) = \psi_{\ell_0}(\frac{1}{15})$. In (b) and (d), we take $\ell_0 = \ell_1 = 8$ and, successively, $p_1 = 1.01$ (not distinguisable from the cubic case); $2; 3; 15$. This means that the interval parameter in the first segment is, successively $\eta_0 = 1.01; 2; 3; 15$, while in the second we have $\eta_1 = \frac{1}{\eta_0}$. In both segments, the corresponding control polygons (symmetric of each other) are obtained with polygon parameters $\psi_8(\eta_0) = \psi_8(\eta_1)$.

Remark 3. Observe that each spline S obtained in this way is automatically C^1. More generally, take any sparsity $\ell > 0$, any positive $p_0 \neq p_1$, and any planar polygons $[Q_0, Q_1, Q_2, Q_3]$ and $[\overline{Q}_0, \overline{Q}_1, \overline{Q}_2, \overline{Q}_3]$ such that $Q_3 = \overline{Q}_0$ is the middle of $[Q_2, \overline{Q}_1]$. Let $Q \in \mathbb{E}(\ell; p_0, p_1)^2$ (resp., $\overline{Q} \in \mathbb{E}(\ell; p_1, p_0)^2$) be defined on $[t_0, t_1]$ (resp., $[t_1, t_2]$) by the control polygon $[Q_0, Q_1, Q_2, Q_3]$ (resp., $[\overline{Q}_0, \overline{Q}_1, \overline{Q}_2, \overline{Q}_3]$). These functions satisfy $Q'(t_1^-) = \overline{Q}'(t_1^+)$ due to (15).

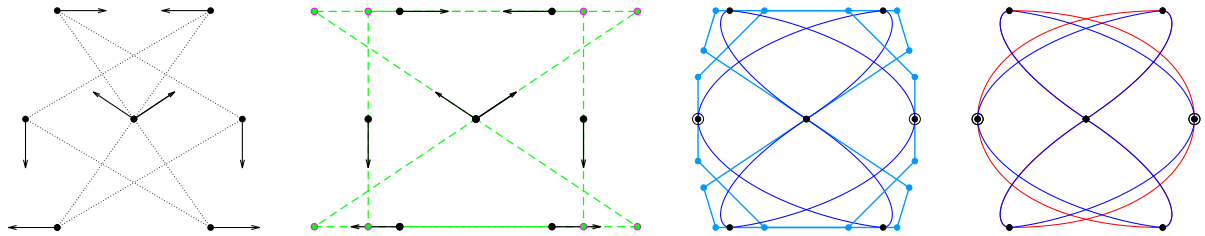

Figure 10: (a) initial tight data (q_k, d_k), $k = 0, \ldots, 8$; (b) the corresponding triangles; (c) for $p_k = 1$ for all k except at the circles where $p_k = 15$, the sparsity being $\ell_k = 8$ in all sections which are not standard cubics, we show the corresponding control polygons and the associated cubic-like sparse G^1 PH-spline interpolant (blue curve); (d) comparison with the standard cubic PH-spline interpolant (red curve).

To definitely illustrate the symmetry preservation, consider the tight data (q_k, d_k), $k = 0, \ldots, 8$, shown in Fig. 10, (a), where q_0 is the central point, and with $q_4 := q_8 := q_0$ and $d_8 := d_0$. The corresponding triangles can be seen in (b). To construct a spline S interpolating these G^1 Hermite data, we complete the information by the knots $t_k = k$ for $k = 0, \ldots, 8$. Assume that all p_k are equal to 1 except those indicated by a circle in (c), (d), where we take the same value. In other words we have $p_2 = p_6$ and $p_k = 1$ for all other k. We thus have to choose $\ell_k = 0$ (or $\eta_k = 1$) for $k = 0, 3, 4, 7$. For each convenient pair (ℓ, p) where ℓ is a non-negative integer and p is a positive number, we complete the data by setting $\ell_k := \ell$ for $k = 1, 2, 5, 6$, and $p_2 = p_6 := p$, given that $p = 1$ if and only if $\ell = 0$. This generates a unique PH-spline S which both interpolates the G^1 data and preserves their symmetry. Apart from the pair $(\ell, p) = (0, 1)$ which produces the unique ordinary cubic PH-spline interpolant, we therefore obtain infinitely many cubic-like sparse PH splines. The interval parameter on $[t_k, t_{k+1}]$ is $\eta_k = p$ for $k = 1, 5$ and $\eta_k = \frac{1}{p}$ for $k = 2, 6$. In both cases the polygon parameter is $\psi_\ell(p)$. For the sake of clarity, in Fig. 10, (c), we show only one example of both all the control polygons and the resulting spline S, obtained with the pair $(\ell, p) = (8, 15)$. Finally, Fig. 10, (d), enables us to compare S (blue curve) with the ordinary cubic PH-spline interpolant obtained with $(\ell, p) = (0, 1)$ (red curve). Note that the two curves coincide on four intervals.

5. G^1 Hermite interpolation by C^1 cubic-like PH-spline curves

The data are the same as in Theorem 4. For the sake of simplicity, from now on we assume that the knots are $t_k = k$, $k = 0, \ldots, r + 1$. Among the infinite number of solutions to the G^1 Hermite interpolation problem (17) – resulting from the parameters inherent in cubic-like sparse spaces (as re-defined in Section 4.2) – can we find one which is C^1 on $[t_0, t_{r+1}] = [0, r + 1]$? We can give an affirmative answer to this question, thus solving the problem

$$\begin{gathered} \textit{Among all solutions } S : [t_0, t_{r+1}] \longrightarrow \mathbb{R}^2 \textit{ to (17), find one such that} \\ \lambda_k^+ = \lambda_k^- \quad \textit{for } k = 1, \ldots, r. \end{gathered} \tag{18}$$

5.1. Mixed C^1/G^1 Hermite interpolation by one cubic-like sparse PH function

In this section we consider only one curve segment. Given a tight pair of planar interpolation data (q_0, d_0), (q_1, d_1), we want to solve a mixed C^1 / G^1 interpolation problem on $I = [0, 1]$, *i.e.*, interpolation point q_0 and exact derivative at 0, interpolation point q_1 and oriented tangent at 1, so as to obtain a

PH-curve. The problem can be formulated as follows:

$$\textit{Find a function } Q : [0,1] \longrightarrow \mathbb{R}^2 \textit{ such that}$$

1) *Q produces a cubic-like sparse PH curve;*

2) *Q satisfies the four interpolation conditions below* (19)

$$\begin{cases} \textit{(i)} & Q(0) = q_0, \\ \textit{(ii)} & Q'(0) = \lambda_0 d_0, \textit{ for a } \underline{\textit{given}} \ \lambda_0 > 0; \end{cases} \qquad \begin{cases} \textit{(iii)} & Q(1) = q_1, \\ \textit{(iv)} & Q'(1) = \lambda_1 d_1, \textit{ for some unknown } \lambda_1 > 0. \end{cases}$$

With a view to repeat this mixed interpolation process to build a solution S to the problem (18), the function Q must be found in some $\mathbb{E}(\ell; p_0, p_1)^2$ and with no loss of generality we can assume that $p_0 > 0$ is given.

As previously we consider the triangle $[A, B, C] := [q_0, q_{0,1}, q_1]$ deduced from the pair of data, and we assume that we are in the situation $\|C - B\| \geqslant \|A - B\|$, so that we are exactly in the situation depicted in Fig. 6. The ordinary cubic space (obtained for $p_1 = p_0$ and $\ell = 0$) provides us with a solution to the problem above if and only if $\lambda_0 = 3\,\|E_1 - q_0\|$. In that case the solution is unique. Subsequently, we exclude this case.

Take any pair (ℓ, p_1), where ℓ is a positive integer, and $p_1 \in]0, +\infty[\setminus\{p_0\}$. If $[E, F]$ is the segment parallel to $[A, C']$ given by (9) where

$$\alpha := \psi_\ell(\eta) \in \,]1, \alpha_\ell^*[\ = \ \left]1, \frac{2\ell+2}{\ell+2}\right[, \quad \text{with } \eta := \frac{p_1}{p_0},$$

the function $Q \in \mathbb{E}(\ell; p_0, p_1)^2$ with control polygon $[q_0, E, F, q_1]$ automatically satisfies the three requirements (i), (iii), and (iv), in (19), and it produces a cubic-like sparse PH curve with sparsity ℓ, interval parameter η, and polygon parameter α. Solving the above problem therefore consists in proving that we can select one among all such pairs (ℓ, p_1), or (ℓ, η) as well, so as to additionally satisfy the missing requirement (ii). Now, according to the left equality in (15), condition (ii) is satisfied if and only

$$\frac{3}{\varphi_\ell(\eta)} \ \|E - q_0\| = \lambda_0. \tag{20}$$

The function φ_ℓ is strictly increasing on $[0, +\infty[$, and it satisfies $\varphi_\ell(0) = \frac{3}{\ell+3}$ (see Lemma 3 in [7]). Accordingly, for (20) to be satisfied, it is necessary that

$$\ell + 3 > \frac{\lambda_0}{\|E_1 - q_0\|}. \tag{21}$$

By comparison, below we can state a simple sufficient condition ensuring the solvability of (19).

Proposition 5. *There exist infinitely many solutions to the mixed interpolation problem (19). More precisely, each sparsity ℓ satisfying*

$$\ell + 3 \geqslant \frac{\lambda_0}{\|E_2 - q_0\|} \tag{22}$$

provides us with a solution to (19).

Proof. For each $\alpha > 0$, let $[E_\alpha, F_\alpha]$ denote the segment such that the polygon $[q_0, E_\alpha, F_\alpha, q_1]$ has polygon parameter α and satisfies $\theta_1 = \theta_2$. Solving (20) amounts to solving the following problem:

$$\begin{gathered} \textit{Find } \eta \in]0, +\infty[\setminus\{1\} \textit{ such that } \varphi_\ell(\eta) = H_\ell(\eta), \ \textit{where } H_\ell \textit{ is defined on } [0, +\infty[\textit{ by} \\ H_\ell(\eta) := \frac{3}{\lambda_0} \ \left\|E_{\psi_\ell(\eta)} - q_0\right\|. \end{gathered} \tag{23}$$

Observe that

$$H_\ell(1) = \frac{3}{\lambda_0}\,\|E_1 - q_0\| > H_\ell(0) = \frac{3}{\lambda_0}\,\|E_\ell^* - q_0\| > \frac{3}{\lambda_0}\,\|E_2 - q_0\|. \tag{24}$$

η	0	1	$+\infty$
$\psi_\ell(\eta)$	α_ℓ^* ↘	1	↗ α_ℓ^*
$H_\ell(\eta)$	$H_\ell(0)$ ↗	$H_\ell(1)$	↘ $H_\ell(0)$
$\varphi_\ell(\eta)$	$\frac{3}{\ell+3}$ ↗	1	↗ $+\infty$

Table 1: On $[0, +\infty[$, joint variations of the functions ψ_ℓ, φ_ℓ, and of the function H_ℓ defined in (23).

Let a positive sparsity ℓ satisfy (22). From (24) we can then derive that

$$H_\ell(0) > \frac{3}{\ell+3}.$$

Since we have excluded the cubic case, we know that $H_\ell(1) \neq 1$. Comparison of the variations of the two functions φ_ℓ and H_ℓ on $[0, +\infty[$ (see Table 1), shows that there exists always a solution to (23). More precisely, if $H_\ell(1) > 1$, exactly one value of $\eta > 1$ satisfies $\varphi_\ell(\eta) = H_\ell(\eta)$, while if $H_\ell(1) < 1$, there exists a solution on $]0, 1[$. □

Remark 4. Assuming that $\|q_{0,1} - q_0\| \leqslant \|q_1 - q_{0,1}\|$, and with the notations introduced in (9), we can say that

$$H_\ell(\eta) = \frac{2ab^2}{ac\psi_\ell(\eta) + 2b^2 + \sqrt{a\psi_\ell(\eta)\big[ac^2\psi_\ell(\eta) + 4b^2(a+c)\big]}}, \quad \text{for each } \eta > 0,$$

the meaning of a, b, c being the same as in (9). This expression can easily be adapted to the symmetric case where $\|q_{0,1} - q_0\| \geqslant \|q_1 - q_{0,1}\|$.

5.2. Solving the problem (18)

As a consequence of Proposition 5, we can state:

Theorem 6. *There exist infinitely many C^1 cubic-like sparse PH splines S which are solutions to (18).*

Proof. By repeated application of Proposition 5, we can indeed build infinitely many different C^1 cubic-like sparse PH splines $S : [t_0, t_{r+1}] \longrightarrow \mathbb{R}^2$ interpolating the G^1 Hermite data. We successively construct the restriction S_k of S to $[t_k, t_{k+1}]$. For $k = 0$, we first select any positive λ_0, p_0. While the choice of p_0 has no influence on the resulting S, the selected positive number λ_0 will provide us with the quantity $\|S'(t_0)\| = \lambda_0$. We construct S_0 on $[t_0, t_1] = [0, 1]$ by solving the mixed C^1/G^1 interpolation problem (19). This yields infinitely many different functions S_0. Among them, we have the unique cubic PH interpolant to the G^1 data (q_0, d_0) and (q_1, d_1), obtained for one specific value of the positive parameter λ_0, namely $\lambda_0 = 3\,\|E_1 - q_0\|$ (to which corresponds the interval parameter $\eta_0 = 1$, and $p_1 := p_0$). Each other value of λ_0 provides with infinitely many different S_0 depending on the selected sparsity ℓ_0 satisfying (22). For each such sparsity, solving the corresponding equation (23) yields an interval parameter $\eta_0 \in]0, +\infty[\setminus\{1\}$, and the corresponding $S_0 \in \mathbb{E}(\ell_0; p_0, p_1)^2$, with $p_1 := \eta_0 p_0$, determined by its control polygon with polygon parameter $\psi_{\ell_0}(\eta_0)$.

Given an integer k, with $1 \leqslant k \leqslant r$, suppose that we have constructed the functions $S_0, \ldots, S_{k-1}$ along with the positive numbers p_i up to $i = k$. In the triangle $[q_k, q_{k,k+1}, q_{k+1}]$ built from the tight data (q_k, d_k), (q_{k+1}, d_{k+1}), we denote by $[E_1^k, F_1^k]$ and $[E_2^k, F_2^k]$ the two parallel segments indicating the band within which we can obtain PH-curves on $[t_k, t_{k+1}] = [k, k+1]$. We then solve the corresponding mixed C^1/G^1

interpolation problem (19) obtained by replacing $[0,1]$ by $[k,k+1]$, the pair (q_0,d_0), (q_1,d_1), by the pair (q_k,d_k), (q_{k+1},d_{k+1}), p_0 by p_k, and λ_0 by

$$\lambda_k := {S_{k-1}}'(t_k) = {S_{k-1}}'(k).$$

Except when this problem produces the unique cubic PH interpolant to the G^1 tight data (q_k,d_k) and (q_{k+1},d_{k+1}), that is, when $\lambda_k = 3\left\|E_1^k - q_k\right\|$, we obtain infinitely many different functions S_k, depending on the infinitely many possible sparsities. If ℓ_k is one of them, the interval parameter η_k will be obtained by solving the analogue of (23). With $p_{k+1} = \eta_k p_k$, $S_k \in \mathbb{E}(\ell_k; p_k, p_{k+1})^2$ is determined by the fact that its control polygon $[q_k, E^k_{\psi_{\ell_k}(\eta_k)}, F^k_{\psi_{\ell_k}(\eta_k)}, q_{k+1}]$ has interval parameter $\psi_{\ell_k}(\eta_k)$, with $[E^k_{\psi_{\ell_k}(\eta_k)}, F^k_{\psi_{\ell_k}(\eta_k)}]$ parallel to $[E_1^k, F_1^k]$. □

5.3. Illustrations

In this subsection we present three examples of tight data taken from classical parametric curves. In each case, we build a solution to the C^1 interpolation problem (18) through the progressive method described in the proof of Theorem 6. For each $k = 0,\dots,r$, if we are not in the cubic case, the sparsity will systematically be selected as the smallest positive integer ℓ_k satisfying the corresponding sufficient condition (22).

Example 2. In Fig. 11, (a), the fourteen data (q_k,d_k), $k = 0,\dots,r+1 = 13$, are taken from a spiral. As is clear from (a), the initial point q_0 is the external extreme point of the spiral. The selected value for the parameter λ_0 is $\lambda_0 = 0.5$. Selecting all sparsities as explained above yields the sequence

$$(\ell_0,\dots,\ell_{12}) = (1,2,1,2,1,2,1,2,1,2,1,2,1),$$

and the corresponding sequence of interval parameters

$$(\eta_0,\dots,\eta_{12}) \approx (12.1498, 0.3815, 4.7148, 0.4365,\\ 3.7392, 0.4627, 3.3779, 0.4793, 3.1792, 0.4880, 3.0737, 0.4926, 3.0270).$$

This gives the sequence of cubic-like sparse spaces $\mathbb{E}(\ell_k; p_k, p_{k+1})$ on $[t_k, t_{k+1}]$, $k = 0,\dots,12$, providing the successive functions S_k. In Fig. 11, (b), we show the triangle deduced from any two consecutive data (q_k,d_k), (q_{k+1},d_{k+1}). Fig. 11, (c), presents the associated control polygons, determined by their polygon parameters $\psi_{\ell_k}(\eta_k)$, $k = 0,\dots,12$. Finally, Fig. 11, (d), shows the graph of the resulting C^1 cubic-like sparse PH-spline $S : [0,13] \longrightarrow \mathbb{R}^2$ solution to (18).

Example 3. In this example, the data (q_k,d_k), $k = 0,\dots,r+1 = 20$, shown in Fig. 12, (a), are taken from a Lissajous curve, with

$$q_{10} = q_0, \qquad (q_{20}, d_{20}) = (q_0, d_0),$$

the initial point q_0 being the central point. By comparison with the previous example, not only do we have "closed" data, but these data possess symmetry properties, with two symmetry axes, the horizontal and vertical lines through q_0. We are therefore interested not only in obtaining a C^1 cubic-like sparse PH spline S on $[t_0,t_{20}] = [0,20]$, but also in both preserving the symmetry properties of the data, and obtaining a C^1 joint at $q_0 = q_{20}$. This will be made possible by extending the arguments used in Section 4.3.

Since all other data can be deduced by symmetry from the six pairs (q_k,d_k), $k = 0,\dots,5$, it is sufficient to solve the interpolation problem (18) involving only these pairs. Suppose indeed that we have built a solution $\overline{S} : [0,5] \longrightarrow \mathbb{R}^2$ to the latter problem. This C^1 function $\overline{S}$ is characterised by two sequences, namely the sequence $(\ell_0,\ell_1,\ell_2,\ell_3,\ell_4)$ of sparsities on the five intervals concerned, and the sequence $(p_0,p_1,p_2,p_3,p_4,p_5)$ of positive numbers, where p_0 can be chosen arbitrarily. These two sequences determine the sparse spaces $\mathbb{E}(\ell_k; p_k, p_{k+1})$, $k = 0,\dots,4$, providing the functions defining the PH segments. Setting

$$\begin{aligned}(\ell_0,\dots,\ell_{19}) &:= (\ell_0,\ell_1,\ell_2,\ell_3,\ell_4,\ell_4,\ell_3,\ell_2,\ell_1,\ell_0,\ell_0,\ell_1,\ell_2,\ell_3,\ell_4,\ell_4,\ell_3,\ell_2,\ell_1,\ell_0),\\ (p_0,\dots,p_{20}) &:= (p_0,p_1,p_2,p_3,p_4,p_5,p_4,p_3,p_2,p_1,p_0,p_1,p_2,p_3,p_4,p_5,p_4,p_3,p_2,p_1,p_0),\end{aligned} \tag{25}$$

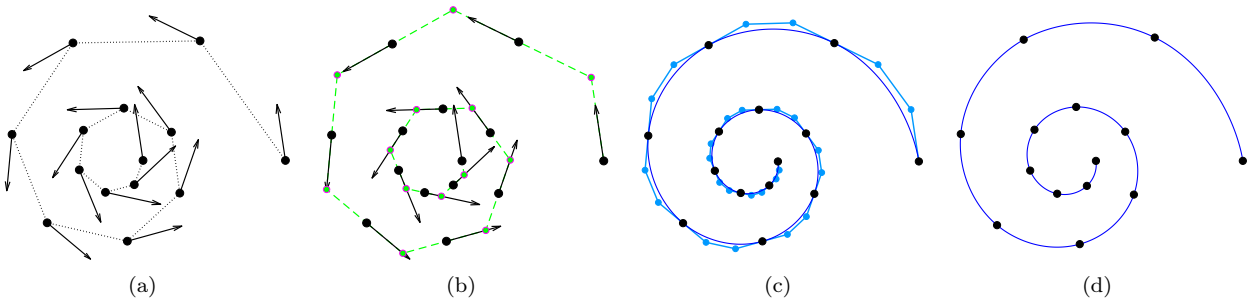

Figure 11: Example 2: (a) initial tight data taken from a spiral; (b) corresponding triangles; (c)-(d) control polygons and C^1 cubic-like sparse PH spline obtained with $\lambda_0 = 0.5$ and sparsities $(\ell_0, \ldots, \ell_{12}) = (1, 2, 1, 2, 1, 2, 1, 2, 1, 2, 1, 2, 1)$.

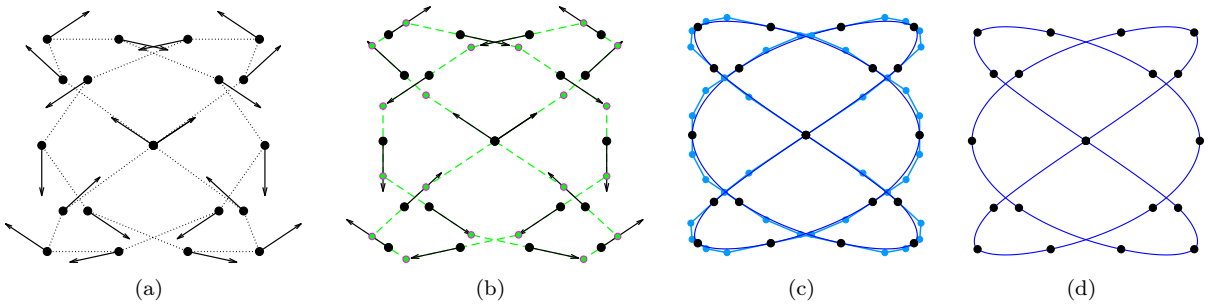

Figure 12: Example 3:(a) initial tight data taken from a spiral; (b) corresponding triangles; (c)-(d) control polygons and C^1 cubic-like sparse PH spline, obtained with $\lambda_0 = 2.6$ and $(\ell_0, \ldots, \ell_4) = (24, 1, 1, 2, 2)$, starting at the central point, and completed so as to preserve the symmetry properties of the data. Entire sequence of sparsities: $(\ell_0, \ldots, \ell_{19}) = (24, 1, 1, 2, 2, 2, 2, 1, 1, 24, 24, 1, 1, 2, 2, 2, 2, 1, 1, 24)$.

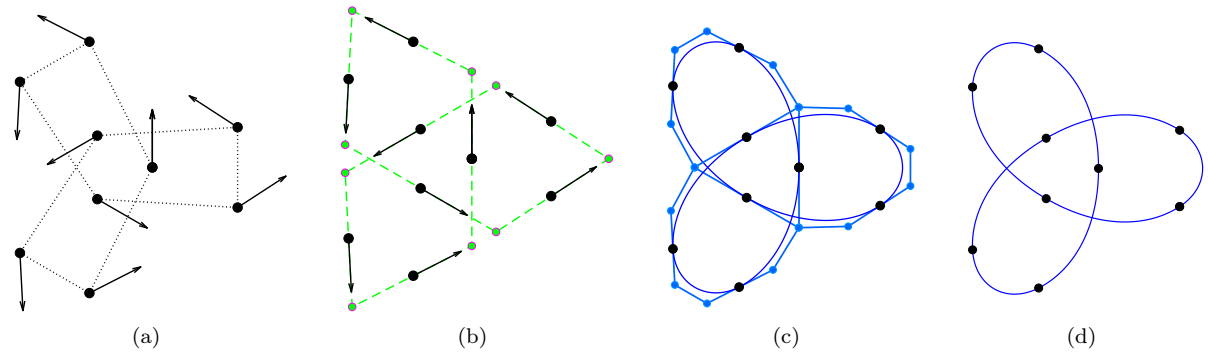

Figure 13: Example 4:(a) initial tight data taken from a knot; (b) corresponding triangles; (c)-(d) control polygons and C^1 cubic-like PH spline, obtained with the initial point q_0 following one of the central points, and $(\ell_0, \ell_1) = (0, 1)$, then completed so as to preserve all symmetry properties of the data. Entire sequence of sparsities: $(\ell_0, \ldots, \ell_8) = (0, 1, 1, 0, 1, 1, 0, 1, 1)$.

provides us with a unique cubic-like sparse PH-spline S on $[0, 20]$. This function is C^1, it guarantees a C^1 joint at $q_0 = q_{20}$, and it preserves all symmetry properties of the data. The reader can get convinced of this by carefully checking the symmetry between the various triangles in Fig. 12, (b), taking account of the formulæ (15) giving the derivatives at the endpoints along with the symmetry permitted by any two cubic-like sparse spaces $\mathbb{E}(\ell; p_0, p_1)$ and $\mathbb{E}(\ell; p_1, p_0)$. In other words, setting

$$(q_{k+20}, d_{k+20}) := (q_k, d_k), \quad \ell_{k+20} = \ell_k, \quad p_{k+20} := p_k, \quad \text{for all } k \in \mathbb{Z},$$

yields a C^1 cubic-like sparse PH-spline defined on the whole real line, with knots at all integers, which interpolates the tight G^1 data (q_k, d_k), $k \in \mathbb{Z}$, and preserves their symmetry properties.

In practice, the function S that we have built, results by applying exactly the same progressive procedure as for the spiral (*i.e.*, on each interval, the sparsity is the least possible integer satisfying the sufficient condition (22)), starting with the parameter $\lambda_0 = 2.6$. This has produced the following two sequences:

$$(\ell_0, \ell_1, \ell_2, \ell_3, \ell_4) = (24, 1, 1, 2, 2); \quad (p_1, p_2, p_3, p_4, p_5) \approx (0.9327, 10.6549, 15, 4485, 10.8062, 20.4378),$$

the right one being obtained with $p_0 := 1$.

Example 4. With $r = 8$ and $(q_9, d_9) = (q_0, d_0)$, we now consider the "closed" G^1 data presented in Fig. 13, (a), taken from a mathematical knot. Because of the symmetry between the three "branches" of the data, the most natural procedure is to do as in the previous example, that is, to consider only one branch and then complete by symmetry. We thus solve the interpolation problem (18) limited to four consecutive data (q_k, d_k), $k = 0, 1, 2, 3$, the initial point q_0 being any of three interior points. Starting from $\lambda_0 = 0.5$, this yields the two sequences

$$(\ell_0, \ell_1, \ell_2) = (1, 2, 1), \qquad (p_1, p_2, p_3) \approx (5.1927, 2.4026, 10.1882),$$

with $p_0 = 1$. To preserve the symmetry of the data on both sides of q_3, and then of q_6, we have to take

$$(\ell_3, \ldots, \ell_8) = (1, 2, 1, 1, 2, 1) \quad (p_0, \ldots, p_9) = (p_0, p_1, p_2, p_3, p_2, p_1, p_0, p_1, p_2, p_3). \tag{26}$$

The resulting cubic-like sparse PH-spline S is certainly C^1 on $[0, 9]$ and it preserves the symmetry between the three branches. However, at $q_0 = q_9$, the joint is not C^1 as is visible on the right sequence in (26) which prevents us from producing the same curve again out of periodicity. The difference with Example 3 lies in the fact that, here, we have an odd number of symmetric branches of data, and only specific choices of the p_k can provide the possibility of extending the associated piecewise function out of periodicity: those ensuring also symmetry between the first and last segments.

In direct connection with this, there is actually another problem concerning the spline S defined by (26): it does not preserve the symmetry existing between the first four data themselves. This symmetry results in the specific configuration of the three triangles $[q_k, q_{k,k+1}, q_{k+1}]$, $k = 0, 1, 2$. The first and third ones are symmetric of each other. As for the central one, it is an isosceles triangle, and the only possibility to preserve its own symmetry consists in choosing the standard cubic PH-curve provided by that triangle.

With this in view, we have to choose q_0 right after an interior point. We define S_0 as the cubic function on $[0, 1]$ with control polygon $[q_0, E_1^0, F_1^0, q_1]$. Then we simply solve the mixed C^1/G^1 interpolation problem (19) on the interval $[1, 2]$, related to the G^1 data (q_1, d_1) and (q_2, d_2), with the parameter $\lambda_1 := S_0'(1)$ fixing the first derivative at 1. Choosing as previously the least possible value satisfying the sufficient condition (22), we take $\ell_1 = 1$, and, if $p_0 = p_1 = 1$, we have $p_2 \approx 1.2378$. All symmetry properties will be preserved with

$$(\ell_0, \ldots, \ell_8) := (0, \ell_1, \ell_1, 0, \ell_1, \ell_1, 0, \ell_1, \ell_1), \quad (p_0, \ldots, p_9) := (p_0, p_0, p_2, p_0, p_0, p_2, p_0, p_0, p_2, p_0), \tag{27}$$

also ensuring the C^1 joint at $q_0 = q_9$.

Remark 5. It is worthwhile commenting on Example 4. Preserving the symmetry within a branch of data has reduced the number of possibilities, since we no longer have the initial free parameter λ_0 at our disposal:

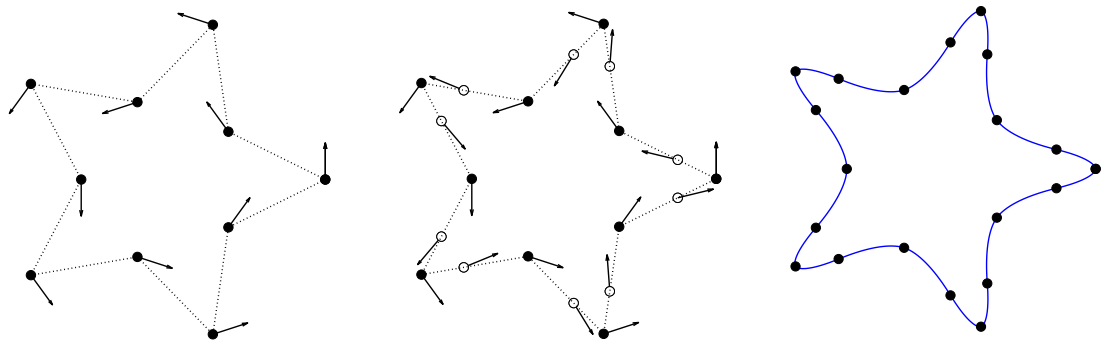

Figure 14: (a) initial non tight data; (b) tight data after pre-processing; (c) the resulting C^1 cubic-like sparse PH spline, obtained with $\lambda_0 = 0.4732$, $(\ell_0, \ell_1) = (1, 8)$ (starting at the extreme point of a branch of the star) and completed by symmetry. Entire sequence of sparsities: $(\ell_0, \dots, \ell_{19}) = (1, 8, 8, 1, 1, 8, 8, 1, 1, 8, 8, 1, 1, 8, 8, 1, 1, 8, 8, 1)$.

only the sparsity $\ell_1 \geqslant 1$ is free. The main advantage is that it makes the extension by periodicity possible. Clearly, had we had to preserve a second symmetry constraint of the same type, obtaining a C^1 PH spline would have been impossible, except by chance, exactly as in the case of cubic PH splines. Imagine, for instance, that the data produce two consecutive isosceles triangles, with same angles but different lengths: then it is impossible to simultaneously respect the symmetry of the triangles and the C^1 joint.

5.4. Non-tight data

In this subsection we briefly remind the reader of the pre-processing step which can be applied to a set of non-tight data in order to transform it into a set of tight data which can then be handled as described in the previous examples. The method that we apply below is taken from [20]. We explain it on one example of "closed" non-tight data (q_k, d_k), $k = 0, \dots, 10$, shown in Fig. 14, (a), with $(q_{10}, d_{10}) = (q_0, d_0)$. We first extend the data by setting $(q_{k+10}, d_{k+10}) := (q_k, d_k)$ for all $k \in \mathbb{Z}$. Clearly any pair (q_k, d_k), (q_{k+1}, d_{k+1}) are non-tight. We rename all data as

$$\left(\widetilde{q}_{2k}, \widetilde{d}_{2k}\right) := (q_k, d_k), \quad k \in \mathbb{Z}.$$

For $k \in \mathbb{Z}$, we have to define $\left(\widetilde{q}_{2k+1}, \widetilde{d}_{2k+1}\right)$ so that both pairs $\left(\widetilde{q}_{2k}, \widetilde{d}_{2k}\right)$, $\left(\widetilde{q}_{2k+1}, \widetilde{d}_{2k+1}\right)$ and $\left(\widetilde{q}_{2k+1}, \widetilde{d}_{2k+1}\right)$, $\left(\widetilde{q}_{2k+2}, \widetilde{d}_{2k+2}\right)$ will be tight. Due to the symmetry and periodicity properties of the data, here it is sufficient to do it with $k = 0$. Then, the point $\widetilde{q}_1$ is obtained by intersecting the segment $[q_0, q_1] = [\widetilde{q}_0, \widetilde{q}_2]$ and the cubic Lagrange interpolant to the four points q_{-1}, q_0, q_1, q_2, and the tangent direction to this interpolant at $\widetilde{q}_{2k+1}$ is taken as $\widetilde{d}_{2k+1}$. The new data $\left(\widetilde{q}_k, \widetilde{d}_k\right)$, $k \in \mathbb{Z}$, shown in Fig. 14, (b), are tight. We can then proceed as usual. [2]

Due to the symmetry properties of the data, it is actually sufficient to solve the interpolation problem (18) with only the data $\left(\widetilde{q}_0, \widetilde{d}_0\right)$, $\left(\widetilde{q}_1, \widetilde{d}_1\right)$, $\left(\widetilde{q}_2, \widetilde{d}_2\right)$. If a given solution to this problem is described by the sparisties (ℓ_0, ℓ_1) and the positive numbers (p_0, p_1, p_2), a global C^1 interpolant is obtained with the two infinite sequences

$$(\dots, \ell_0, \ell_1, \ell_1, \ell_0, \ell_0, \ell_1, \ell_1, \ell_0, \dots), \quad (\dots, p_0, p_1, p_2, p_1, p_0, p_1, p_2, p_1, p_0, \dots).$$

[2] Most of the time the method described above produces tight data, as is the case in Fig. 14. However, if it is not so, other methods can be used. For instance, the new point $\widetilde{q}_{2k+1}$ can be defined as the midpoint of $[q_k, q_{k+1}]$, and the associated direction $\widetilde{d}_{2k+1}$ is then selected appropriately [20].

Selecting the initial point $\widetilde{q}_0 = q_0$ at the extremity of a branch of the polygon, and with $\lambda_0 = 0.5$, we obtain $(\ell_0, \ell_1) = (1, 8)$, and with $p_0 := 1$, $(p_1, p_2) \approx (0.6917, 0.7565)$. This corresponds to the curve presented in Fig. 14, (c).

6. Final comments

Replacing cubic spaces by the larger framework of cubic-like sparse spaces has enabled us to construct C^1 PH spline functions interpolating given tight G^1 Hermite data, and based on given knot-vectors. This is due to the free parameters involved in cubic-like sparse spaces, which even permit to obtain infinitely many solutions to such interpolation problems. The method presented in this article is progressive: we construct the C^1 cubic-like sparse PH spline function piece after piece, in order to ensure a C^1 joint between consecutive pieces, depending on an initial free parameter and on the selected sparsities.

Cubic-like sparse spaces do not preserve the possible symmetry of control polygons. Nevertheless, save for exceptional configurations (see Remark 5), a suitable use of these spaces can permit to construct the C^1 PH spline function so as to preserve the symmetry properties of the given tight G^1 data, if any. Again, this may even be done in infinitely many different ways. The examples investigated indicate how to possibly handle the symmetry properties to obtain a C^1 closure in case the data themselves are closed.

At the moment, how can we obtain C^1 closure when it is not possible to deduce it from symmetry remains an open problem. To solve it, it might be necessary to replace the progressive method by a global treatment of this issue. Other interesting issues on cubic-like sparse PH splines, to be addressed in the future, are the investigation of their approximation order and the construction of spatial splines interpolating G^1 data. Besides, it is known that C^1 can be obtained with ordinary PH-splines provided that we increase the degree, typically with quintic PH-splines [16]. On account of the advantages permitted by sparse spaces, considering quintic-like sparse PH-splines to ensure higher continuity conditions, such as C^2, is a natural issue. This too will be considered in future work.

The examples addressed in the previous section offer us an opportunity to conclude these final comments with a crucial observation on cubic-like sparse PH curves and splines, and even more on sparse spaces. Indeed, readers can be surprised by the sparsity $\ell_0 = 24$ appearing in Example 3. Certainly, we are then dealing with polynomials of degree 27, but the foremost point to be remembered is that we are in fact dealing with parametric curves controlled by four points with hardly more difficulty than ordinary cubics. For this reason, the value $\ell_0 = 24$ is not a problem. Nonetheless, we would like to stress that, on purpose, all our examples have been treated through the strong simple sufficient condition (22). We have made no special effort to lower this value of ℓ_0 although it would have been very easy through weaker sufficient conditions. For instance, Table 1 makes it obvious that, had we chosen the free parameter λ_0 so that $\lambda_0 < 3\,\|E_1 - q_0\|$, any positive sparsity would have ensured a solution to the corresponding crucial equation (23). Accordingly, we could have taken $\ell_0 = 1$, keeping in mind that this would have had an impact on all other sparsities. In most cases, we can do better (in the sense of lower degree) that the results presented: as an instance, the star data (Example 5.4) does produce a C^1 cubic-like sparse PH spline interpolant preserving all symmetry properties of the data with all sparsities equal to 1.

Acknowledgements

The second author gratefully acknowledges support from INdAM-GNCS Gruppo Nazionale per il Calcolo Scientifico, Italy.

References

[1] Ait-Haddou, R., Biard, L. (1994). G^2 approximation of an offset curve by Tschirnhausen quartics. In *Mathematical Methods for Curves and Surfaces*, Vanderbilt University Press, 1–10.

[2] Ait-Haddou, R., Herzog, W., Biard, L. (2008), Pythagorean-hodograph ovals of constant width. Computer Aided Geometric Design 25, 258–273.

[3] Ait-Haddou, R., Sakane, Y., Nomura, T. (2013). Chebyshev blossoming in Müntz spaces: toward shaping with Young diagrams, Journal of Computational and Applied Mathematics, 247, 172–208.
[4] Ait-Haddou, R., Sakane, Y., Nomura, T. (2013). Gelfond-Bézier curves. Computer Aided Geometric Design, 30, 199-225.
[5] Ait-Haddou, R. (2014). Dimension elevation in Müntz spaces: A new emergence of the Müntz condition, Journal of Approximation Theory, 181, 6–17.
[6] Ait-Haddou, R., Mazure, M.-L. (2013). Approximation by Müntz spaces on positive intervals. Comptes Rendus Mathématique, 351, 849–852.
[7] Ait-Haddou, R., Mazure, M.-L. (2017). Sparse Pythagorian hodograph curves, Computer Aided Geometric Design, 55, 84–103.
[8] Albrecht, G., Beccari, C.V., Canonne, J.-C., Romani, L. (2017). Planar Pythagorean-hodograph B-spline curves. Computer Aided Geometric Design, 57, 57–77.
[9] Bastl, B., Slabá, K., Byrtus., M. (2013). Planar C^1 Hermite interpolation with uniform and non-uniform TC-biarcs, Computer Aided Geometric Design, 30, 58–77.
[10] Choi, H. I., Farouki, R.T., Kwon, S.-H., Moon, H.P. (2008). Topological criterion for selection of quintic Pythagorean-hodograph hermite interpolants, Computer Aided Geometric Design, 25, 411–433.
[11] Fang, L., Wang, G. (2018). Geometric characteristics of planar quintic Pythagorean-hodograph curves, Journal of Computational and Applied Mathematics, 330, 117–127.
[12] Farouki, R.T. (2008). *Pythagorean-Hodograph Curves: Algebra and Geometry Inseparable*, Springer, Berlin.
[13] Farouki, R.T. (2019). Existence of Pythagorean-hodograph quintic interpolants to spatial G^1 Hermite data with prescribed arc lengths, Journal of Symbolic Computation, 95, 202–216.
[14] Farouki, R.T., Giannelli, C., Sestini, A. (2019). New Developments in Theory, Algorithms, and Applications for Pythagorean-Hodograph Curves. In *Advanced Methods for Geometric Modeling and Numerical Simulation*, Springer INdAM Series, 35, 127–177.
[15] Farouki, R.T., Manjunathaiah, J., Jee, S. (1998). Design of rational CAM profiles with Pythagorean-hodograph curves, Mechanism and Machine Theory, 33, 669–682.
[16] Farouki, R. T., Neff, C. A. (1995). Hermite interpolation by Pythagorean hodograph quintics, Mathematics of Computation, 64, 1589–1609.
[17] Farouki, R. T., Sakkalis, T. (1990), Pythagorean hodographs. IBM Journal of Research and Development, 34(5), 736-752.
[18] Gelfond, A.O. (1950). On the generalized polynomials of S. N. Bernstein (in Russian), Izv. Akad. Nauk SSSR, ser. math., 14, 413–420.
[19] Hirschman, I. I., Widder, D. V. (1949). Generalized Bernstein polynomials, Duke Math. Journal, 16, 433–438.
[20] Jaklič, G., Kozak, J., Krajnc, M., Vitrih, V., Žagar, E. (2010). On interpolation by Planar cubic G^2 Pythagorean-hodograph spline curves, Mathematics of Computation, 79, 305-326.
[21] Jüttler, B. (2001). Hermite interpolation by Pythagorean hodograph curves of degree seven, Mathematics of Computation, 70, 1089–1111.
[22] Karlin, S.J, Studden, W.J., *Tchebycheff Systems: with applications in analysis and statistics*, Wiley Interscience, N.Y., 1966.
[23] Kosinka, J., Lávička, M. (2014). Pythagorean Hodograph Curves: A Survey of Recent Advances, Journal for Geometry and Graphics, 18, 23–34.
[24] Kozak, J., Krajnc, M., Rogina, M., Vitrih, V., Pythagorean hodograph cycloidal curves, J. Numerical Math., 23 (2015) DOI: https://doi.org/10.1515/jnma-2015-0023.
[25] Laurent, P.-J., Mazure, M.-L., Maxim V. (1997). Chebyshev splines and shape parameters, Numerical Algorithms, 15, 373–383.
[26] Lyche, T. (1985). A recurrence relation for Chebyshevian B-splines, Constructive Approximation, 1, 155–173.
[27] Mazure, M.-L. (1998). Vandermonde type determinants and blossoming, Advances in Computational Mathematics, 8, 291–315.
[28] Mazure, M.-L. (1999). Blossoming: a geometrical approach, Constructive Approximation, 15, 33–68.
[29] Mazure, M.-L. (1999). Chebyshev spaces with polynomial blossoms, Advances in Computational Mathematics, 10, 219–238.
[30] Mazure, M.-L. (1999). Bernstein bases in Müntz spaces, Numerical Algorithms, 22, 285–304.
[31] Mazure, M.-L. (2001). Chebyshev splines beyond total positivity, Advances in Computational Mathematics, 14, 129–156.
[32] Mazure, M.-L (2004). Blossoms and optimal bases, Advances in Computational Mathematics, 20, 177-203.
[33] Mazure, M.-L. (2012). On a new criterion to decide whether a spline space is suitable for design, BIT Numerical Mathematics, 52, 1009–1034.
[34] Mazure, M.-L., Laurent, P.-J. (1998). Nested sequences of Chebyshev spaces and shape parameters, Mathematical Modeling Numerical Analysis, 32, 773–788.
[35] Mazure, M.-L., Laurent, P.-J. (1999). Polynomial Chebyshev splines, Computer Aided Geometric Design, 16, 317–343.
[36] Meek, D. S., Walton, D. J. (1997). Geometric Hermite interpolation with Tschirnhausen cubics, Journal of Computational and Applied Mathematics, 299-309.
[37] Pelosi, F., Sampoli, M., Farouki, R.T., Manni, C. (2007). A control polygon scheme for design of planar C^2 PH quintic spline curves, Computer Aided Geometric Design, 24, 28–52.
[38] Pottmann, H. (1993). The geometry of Tchebycheffian splines, Computer Aided Geometric Design, 10, 181–210.
[39] Pottmann, H. (1995). Curve design with rational Pythagorean-hodograph curves, Advances in Computational Mathematics, 3, 147–170.
[40] L.L. Schumaker, *Spline Functions*, Wiley Interscience, N.Y., 1981.
[41] Schweikert, D.G. (1966). An interpolation curve using a spline in tension, Journal of Mathematical Physics, 45 , 312–317.

[42] Sir, Z., Jüttler, B. (2007). C^2 Hermite interpolation by pythagorean hodograph space curves, Mathematics of Computation,76, 1373– 1391.